# Theory and Application of Fluorescence Homotransfer to Melittin Oligomerization

Loren W. Runnels and Suzanne F. Scarlata

Department of Physiology and Biophysics, State University of Stony Brook, Stony Brook, New York 11794-8661 USA

ABSTRACT Fluorescence homotransfer (electronic energy transfer between identical fluorophores) has the potential to quantitate the number of subunits in membrane protein oligomers. Homotransfer strongly depolarizes fluorescence emission as a result of intermolecular excitation energy exchange between an initially excited, oriented molecule and a randomly oriented neighbor. We have theoretically treated fluorescein labeled subunits in an oligomer as a cluster of molecules that can exchange excitation energy back and forth among the subunits within that group. We find that the larger the number of subunits, the more depolarized is the emission. The general equations to calculate the expected anisotropy for complexes composed of varying numbers of labeled subunits are presented. Self-quenching of fluorophores, orientation, and changes in lifetime are also discussed and/or considered.

To test this theory, we have specifically labeled melittin on its N-terminal with fluorescein and monitored its monomer to tetramer equilibrium both in solution and in lipid bilayers. The calculated anisotropies are close to the experimental values when non-fluorescent fluorescein dimers are taken into account. Our results show that homotransfer may be a promising method to study membrane-protein oligomerization.

## INTRODUCTION

Many proteins exist as oligomers, and changes in their oligomeric state can have a direct effect on function. Determining the number of subunits in a protein complex usually involves chromatographic or sedimentation methods to quantitate the shape and size of the complex, and electrophoretic methods to determine the different polypeptide chains that make up the complex. For membrane proteins, characterization of the oligomeric state is problematic because it is difficult to isolate the size of the protein complexes from the surrounding lipid. Usually, proteins are solubilized in a gentle, nondenaturing detergent so that traditional techniques can be used to determine subunit number (e.g., GLUT1; Herbert and Carruthers, 1991) and Band 3 (Casey and Reithmeier, 1991). In some cases, success has been achieved using neutron bombardment (for a review, see Timmins and Zaccai, 1988) and antibodies that recognize a particular oligomeric form (e.g., Herbert and Carruthers, 1992). Recent studies using triplet state anisotropy decay show that this technique is sensitive to the self-association of Ca-ATPase (Voss et al., 1994) and may be generally applicable to view protein associations in fluid phase membranes, although contributions of annular lipid to the rotational volume must be considered.

In this study, we examine an alternative method that has the potential of viewing real time changes in the oligomeric state of proteins embedded in membranes. The method involves nonradiative energy transfer between fluorescein labels on protein subunits. In contrast to electronic energy transfer between different probes where one type of molecule acts as an energy "donor" and the other acts as an energy "acceptor," in homotransfer fluorescein is both donor and acceptor. Energy transfer between identical fluorescein species has the potential to resolve oligomers composed of more than two subunits. As is the case for heterotransfer, in homotransfer the probes must be within a critical distance of each other, and the emission energy spectrum of the donor must sufficiently overlap with the absorption energy spectrum of the acceptor. Thus, probes with a small Stokes shift will have a greater probability of homotransfer than probes with a large Stokes shift. Fluorescein has a high potential for homotransfer because of its small Stokes shift (see Fig. 1), high quantum yield, and large extinction coefficient.

Homotransfer analysis has been applied to determine the number of probe binding sites in BSA (Weber and Daniels, 1966) and to monitor the dissociation of oligomeric proteins under high pressure (Erijman and Weber, 1991). Although these studies were instrumental in estimating the percent change in the number of transferring species through statistical analyses, they did not rigorously treat homotransfer data by allowing for the effects of fluorophore self-quenching or anisometrical mutual separation distances of the fluorophores relative to one another.

In this study we develop a general expression for homotransfer between fluorescein residues attached to protein subunits, taking into account factors that may alter the observed anisotropy, and treating the oligomers as clusters possessing a defined number of transferring species. We first present a discussion of the theoretical background of this problem in the context of resolution of subunit number using cluster theory, as originally introduced by Knox (1968b), and develop general expressions for the detection of homotransfer by fluorescence anisotropy, taking into account rotational fluorescence depo-
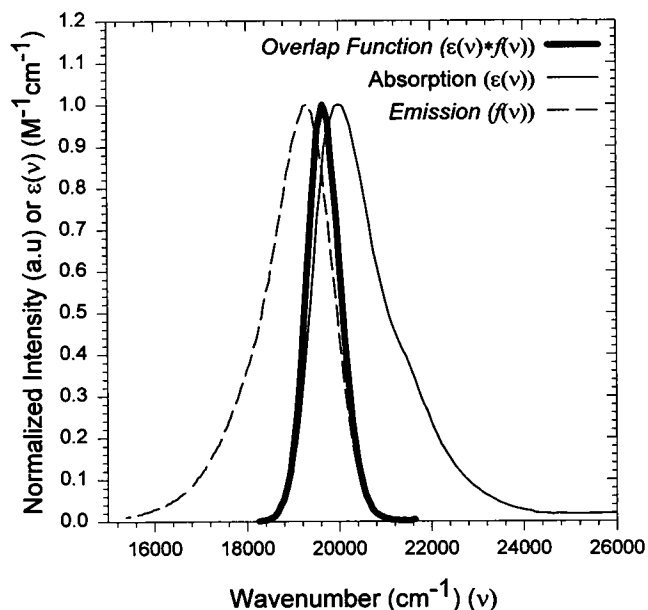
FIGURE 1 Normalized absorption (*thin solid line*) and emission spectrums (*dashed line*) of fluoresceinylated melittin (F-melittin) in 50 mM MOPS, pH 7.2. From Förster's theory, the sixth power of the critical separation distance ($R_o^6$) is directly proportional to the extent of overlap of the absorption and emission spectrum, shown here as the overlap function (*thick solid line*). Using these spectra we calculated a value of approximately 53 Å for $R_o$.

larization. We then present results for a homotransfer study of a model peptide system.

The model system we have studied is melittin. Melittin is a 26-residue peptide, whose structure, oligomerization, and membrane binding properties have been well characterized (for a review see Dempsey, 1990). Melittin contains many positively charged residues that allow for strong interactions with lipid membranes. In aqueous solution, melittin exists in a random coil conformation. Under conditions where charge repulsion is reduced by increasing the ionic strength or raising the pH, melittin will form $\alpha$-helical tetramers at sufficient concentrations. Ionic shielding need not be extensive, because even modification of the N-terminus substantially promotes oligomerization (Lauterwein et al., 1980; Hagihara et al., 1992). The crystal structure of the melittin tetramer has been solved, and the relative positions of the amino acid side chains are known (Terwilliger and Eisenberg, 1982). The N-terminal of the tetramer has a $pK_a$ distinct from the lysine residues (Dempsey, 1990, and references therein), which allows us to specifically label this site with fluorescein isothiocyanate (FITC). Here, we show that homotransfer can be used to follow the oligomerization of labeled melittin in solution and in membranes, and that homotransfer may be generally suited to study the oligomerization of membrane proteins.

## MATERIALS AND METHODS

Melittin, purchased from Sigma Chemical Company (St. Louis, MO), was further purified using reverse-phase HPLC on a $C_{18}$ column (Goto and Hagihara, 1992). Fractions were collected on an acetonitrile/$H_2O$ gradient, in the presence of 0.1% trifluoroacetic acid, and then lyophilized. Samples were reconstituted in filtered distilled $H_2O$, and concentrations were determined from absorption at 280 nm using a molar extinction coefficient of $\epsilon_{280} = 5570$ $M^{-1}cm^{-1}$, and a molecular weight of 2840 g/mol (Quay and Condie, 1983). Fluorescein-5-isothiocyanate (FITC) was purchased from Molecular Probes (Eugene, OR); an extinction coefficient of 76,000 $M^{-1}cm^{-1}$ at 493 nm, pH 10, was used (Haugland, 1992). Trypsin was obtained from Sigma Chemical Company. All lipids were purchased from Avanti Polar Lipids, Inc. (Alabaster, AL). Large unilamellar vesicles (LUVs) of palmitoyl-2-oleoyl-*sn*-glycero-3-phosphorylcholine (POPC) were prepared by first solubilizing the lipids in chloroform, followed by drying under nitrogen and then under vacuum. Lipids were hydrated by 10 cycles of freeze-thawing using 0.1 M MOPS (pH 7.2) and then extruded through a 0.1-$\mu$m filter.

Steady-state and time-resolved fluorescence measurements were performed on an I.S.S. K2 spectrofluorometer (ISS, Champaign, IL). Solutions were excited at 480 nm. For anisotropy measurements, fluorescence emission was observed at 520 nm, using an Oriel bandpass filter (Stratford, CT). All samples had an optical density of less than 0.05 at the excitation wavelength to avoid inner filter effects. Emission spectra were taken with the excitation polarizer at 0° from vertical and the emission polarizer at 54.7° from vertical, to obtain a polarization-independent emission spectrum. A limiting anisotropy of 0.350 was measured for FITC attached to melittin (F-melittin) by first dissolving F-melittin in a 75% (v/v) glycerol solution with 12 mM MOPS, pH 7.2, 1.0 M sodium chloride, and then cooling to $-70°C$. When the contribution of light scattering was more than 1% of the signal, as was the case for the lipid studies, the samples were corrected by subtracting the background signal from buffer and lipid at identical concentrations under identical optical conditions.

Sequence analysis of F-melittin was performed on an Applied Biosystems 475A protein sequencer (Foster City, CA). Some of the mathematical calculations were aided by Mathcad 4.0 (Math Soft, Inc., Cambridge, MA).

## N-Terminal fluorescein labeling of melittin

FITC reacts specifically with primary and secondary amines in their deprotonated state. Melittin contains several residues that can react with FITC, and it would be advantageous for this study to label melittin on a specific site. NMR studies have estimated the $pK_a$ of the N-terminal glycine (Gly-1) to be between 7.0 and 8.0, and that of the three other lysines (Lys-7, Lys-21, and Lys-23) to be above 9.0 (Dempsey, 1990, and references therein). This difference in $pK_a$ allows us to target FITC labeling to the N-terminal. To specifically label Gly-1, we reacted melittin at pH 6.15 where a population of the N-terminals will be deprotonated and reactive, and where the three Lys would be almost completely protonated and effectively unreactive.

FITC was reacted in 50 mM MES buffer, pH 6.15, for 30 min at a molar ratio of 5:1 FITC:melittin. The reaction was quenched by injecting the solution onto the $C_{18}$ HPLC column. Unreacted melittin and FITC eluted off at about the same time, within a minute, followed 10 min later by one major reaction peak, and three minor reaction peaks, each separated by about 3 min. All four reaction peaks contained fluorescein, as determined by fluorescence. The major reaction peak was collected, lyophilized, and then reconstituted into filtered distilled water. The concentration of fluoresceinylated melittin (F-melittin) was determined using a BCA assay (Pierce, Rockford, IL), using unreacted melittin as a standard. Amino acid sequence analysis of the major reactant fraction yielded the primary sequence of melittin. Sequence analysis indicated that at least 96% of the FITC was attached to the N-terminal glycine. We did not determine the fluorescein position of the remaining 4%.

To ensure that melittin was not doubly labeled we compared the limiting anisotropy of trypsin-digested melittin (described below) and undigested melittin, according to the protocol described above. If two fluorescein moieties are attached to melittin, the limiting anisotropy will be significantly lower than the limiting anisotropy of singularly fluoresceinylated melittin because of energy transfer. We measured nearly identical limiting

anisotropies for both F-melittin samples and free FITC (~0.350), confirming that F-melittin had been fluoresceinylated only once. For the trypsin digestion of F-melittin, we applied trypsin at a 10:1 (w/w) ratio of trypsin to melittin, in 10 mM MOPS, pH 7.2, 1 mM calcium chloride, and allowed the reaction to proceed for more than 30 min.

## Determining the emission anisotropy after transfer ($r_{et}$)

Electronic energy transfer from a donor molecule to an acceptor molecule strongly depolarizes the emission anisotropy from the acceptor molecule when both molecules are randomly oriented with respect to an arbitrary axis. We have attempted to measure the extent of the fluorescence depolarization for the case in which the two participating fluorophores are not completely randomly oriented but are rotationally restricted by the peptide linkage that connects them. We measured the emission anisotropy resulting from a dansyl acceptor molecule attached to the N-terminal of melittin (using the same labeling procedure as described above), with the donor being melittin's sole tryptophan (Trp-19). Preliminary results substantiate the assumption that a single energy transfer event heavily depolarizes the emission anisotropy from the energy acceptor. A precise measurement of the emission anisotropy could not be obtained because of difficulties encountered with solvent shifts of dansyl's absorption and emission spectra. We are now extending our efforts to more quantitatively measure the fluorescence depolarization after energy transfer ($r_{et}$) using multilabeled melittin that is aggregated in solution and in membranes.

## Determination of $R_o$

A quantitative expression for the rate of energy transfer from donor to acceptor ($k_T$) was first derived by Förster (translated version: Förster, 1993):

$$k_T = \frac{1}{\tau_D} \cdot \left(\frac{R_o}{R}\right)^6. \quad (1)$$

Here $\tau_D$ is the average lifetime of the excited donor in the absence of acceptor, and $R$ (cm) is the mutual separation distance between donor and acceptor. A critical distance ($R_o$) exists that represents the mutual separation distance between donor and acceptor at which the rate of energy transfer is equal to the decay rate of the donor in the absence of the acceptor (Steinberg, 1971, and references therein):

$$R_o^6 = \frac{9000 \cdot \ln 10 \cdot \kappa^2 \cdot \phi_D}{128 \cdot \pi^5 \cdot n^4 \cdot N} \int_0^\infty \frac{f_D(\nu) \cdot \epsilon_A(\nu)}{\nu^4} \cdot d\nu. \quad (2)$$

To evaluate this expression for $R_o$, we have assigned $\nu^{-4}$ an average value and taken it out of the integral. Here, $\nu$ is the energy in wave numbers (cm$^{-1}$), $\epsilon_A(\nu)$ (M$^{-1}$cm$^{-1}$) is the molar extinction coefficient of the acceptor, $f_D(\nu)$ is the spectral distribution of donor fluorescence (normalized to unity on a wavenumber scale), $N$ is Avogadro's number, $n$ is the index of refraction of the medium, and $\phi_D$ is the donor's quantum yield in the absence of an acceptor. The parameter $\kappa^2$ is an orientation factor, describing the angular alignment between the emission dipole moment of the donor and the absorption dipole moment of the acceptor. The average value for a random directional distribution is $\kappa^2 = \frac{2}{3}$ (Steinberg, 1971).

We calculate an $R_o$ of approximately 56 Å from F-melittin's absorption and fluorescence data for pH 7.2 (see Fig. 1) and an $R_o$ of 57 Å for pH 10.0. Using absorption and anisotropy measurements, we estimate that coupling FITC to melittin decreases FITC's extinction coefficient by roughly 30%. This change merely shifts the values for $R_o$ at pH 7.2 and pH 10.0 to 53 and 54 Å, respectively. These numbers agree well with Craver and Knox's value of 58.2 ± 2.3 Å, although these authors used the notation $\bar{R}_o$ for our $R_o$ (Craver and Knox, 1971). For our calculations, we have used a value of 1.34 for the index of refraction of the solution (Steinberg, 1971), and an average quantum yield of 0.795 for FITC (Weber and Teale, 1957). From

anisotropy measurements of melittin tetramers with only one fluorescein probe, we estimate the rotational mobility of the fluorophore to be very large; therefore, we assumed an average value of $\frac{2}{3}$ for the orientation factor $\kappa^2$ as well.

## BACKGROUND AND THEORY

We will use the term "cluster," as first defined by R. S. Knox, to describe a set of molecules that interact together as a group (Knox, 1968b). Each cluster is isolated and behaves independently. A molecule within a cluster can interact only with its neighbors.

### N = 1 cluster

These molecules have no neighbors. The exponential decay is given by (Förster, 1993)

$$\frac{d\rho(t)}{dt} = -\left(\frac{1}{\tau_o} + Q\right) \cdot \rho(t) \Rightarrow \rho(t) = e^{-t/\tau}\left(\frac{1}{\tau} = \frac{1}{\tau_o} + Q\right). \quad (3)$$

Here, $\rho(t)$ is the probability that the molecule is in the excited state as a function of time, with temporal boundary conditions: $\rho(t = 0) = 1$ and $\rho(t = \infty) = 0$. $\tau$ and $\tau_o$ represent the average lifetime and the natural radiative lifetime of the fluorophore, respectively; and $Q$ describes the source of all nonradiative rates of deexcitation. The quantum yield ($\phi$) is then

$$\phi = \frac{1}{\tau_o} \int_0^\infty \rho(t) \cdot dt = \frac{\tau}{\tau_o}. \quad (4)$$

Thus, if the quantum yield is reduced by any nonradiative process, the result will be a concomitant decrease in the average lifetime.

### N = 2 cluster

For a cluster of two identical molecules undergoing energy transfer (homotransfer), the equations describing the motion of the excitation between them, and its duration, are coupled. For the case of two molecules, $j$ and $k$, with temporal boundary conditions: $\rho_j(t = 0) = 1$, $\rho_j(t = \infty) = 0$, $\rho_k(t = 0) = 0$, and $\rho_k(t = \infty) = 0$ (see Fig. 2), where $t = 0$ represents the time of initial photoexcitation, the probability of molecule $j$ being in the excited state at time $t$ ($\rho_j(t)$) will decay at a rate proportional to $\rho_j(t)$ and the bimolecular transfer rate from $j$ to $k$ ($F_{jk}$), while it increases at a rate proportional to $\rho_k(t)$ and the bimolecular transfer rate from molecule $k$ to $j$($F_{kj}$):

$$\frac{d\rho_j(t)}{dt} = -\frac{\rho_j(t)}{\tau} - F_{jk}\rho_j(t) + F_{kj}\rho_k(t)$$

$$\frac{d\rho_k(t)}{dt} = -\frac{\rho_k(t)}{\tau} - F_{kj}\rho_k(t) + F_{jk}\rho_j(t). \quad (5)$$

FIGURE 2 (a) Sketch of model for a cluster of two, showing the dynamic interactions between molecule $j$ and $k$. Here $F_{jk}$ and $F_{kj}$ are Förster's transfer rates (Eq. 6) for excitation energy transfer (homotransfer) between the molecules. (b) Diagram for a four-molecule cluster. (c) Diagram for a four-molecule cluster in which two of the molecules have engaged to form a nonfluorescent dimer, or "dark complex." Molecules $a$ and $b$ engage in active energy transfer, and the dark complex acts as an energy trap, sapping the excitation energy via a Förster mechanism from molecules $a$ and $b$. The dark complex thus reduces both the quantum yield and fluorescence lifetime of the cluster. A cluster of four possessing two active molecules with one dark complex would essentially behave as a normal cluster of two, because of the reduction of two active fluorophores from excitation energy mixing.
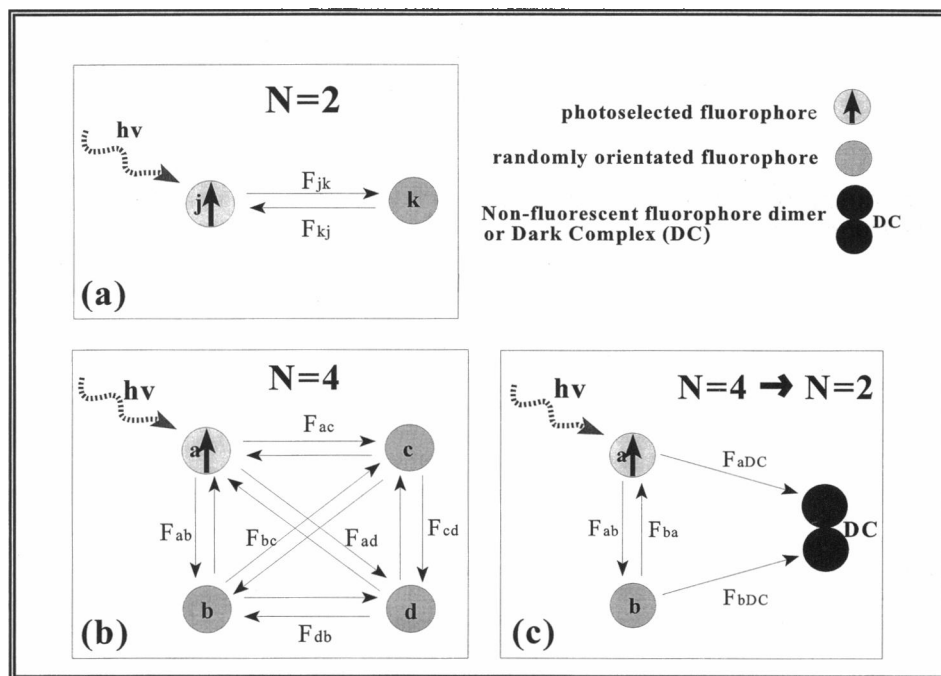


Recalling the right side of Eq. 1, the pairwise excitation transfer rate from molecule $j$ to molecule $k$, or Förster's transfer rate $(F_{jk})$, is given below.

$$F_{jk} = \frac{1}{\tau} \cdot \left(\frac{R_o}{R_{jk}}\right)^6.  \quad (6)$$

Equation 7 shows the original solution to Eq. 5 for $\rho_j(t)$ and $\rho_k(t)$, as given by Förster (1993).

$$\rho_j(t) = \frac{1}{2} \cdot (1 + e^{-2 \cdot F \cdot t}) \cdot e^{-t/\tau}$$
$$\quad\quad\quad\quad\quad\quad\quad (F = F_{jk} = F_{kj}) \quad (7)$$
$$\rho_k(t) = \frac{1}{2} \cdot (1 - e^{-2 \cdot F \cdot t}) \cdot e^{-t/\tau}$$

The sum of the individual decay probabilities, $\rho_j(t)$ and $\rho_k(t)$, represents the decay probability for the whole system or cluster, and is identical to the decay probability for a cluster of one (Eq. 3). The total excitation energy decay rate within the cluster is indistinguishable from the excitation energy decay rate of an isolated molecule. Also, homotransfer does not affect the total quantum yield of the system or cluster, only the quantum yield arising from each individual molecule.

However, energy transfer between identical molecules can decrease the fluorescence anisotropy. Agranovich and Galanin (1982) calculated this effect for the case where the electronic transition dipoles of two molecules are randomly oriented and the excitation light vector is vertically polarized. If the absorption and emission dipoles in each molecule are parallel and the probes do not rotate, the emission anisotropy from the initially excited molecule is 0.4, and the emission anisotropy arising from the second molecule after a single energy transfer event is 0.016. If the individual absorption and emission dipoles are not parallel and the probes can rotate, the fluorescence depolarization is even greater. Therefore, it is typically assumed (i.e., for randomly

oriented molecules) that the fluorescence is fully depolarized after one energy transfer event (as described in Materials and Methods, our preliminary studies support this assumption, but see below). However, with homotransfer there is a finite probability that the excitation energy may be transferred back to the initially excited molecule independently of the initial transfer. This "back-transfer" creates a dynamic system of electronic energy exchange in which equilibrium is established among all the molecules in the cluster. The resulting emission anisotropy is thus composed of two components: the anisotropy from the initially excited molecule and the anisotropy from its neighboring molecules in the cluster that become electronically excited solely by homotransfer. We can calculate the anisotropy for a system containing clusters of two molecules by examining each molecule's quantum yield contribution, $\phi_j$ and $\phi_k$:

$$\phi_j = \frac{1}{\tau_o} \cdot \int_0^\infty \rho_j(t) \cdot dt = \phi_{tot} \cdot \frac{1 + \tau \cdot F}{1 + 2 \cdot \tau \cdot F}$$
$$\quad\quad\quad\quad\quad\quad\quad\quad\quad\quad\quad\quad\quad\quad (8)$$
$$\phi_k = \frac{1}{\tau_o} \cdot \int_0^\infty \rho_k(t) \cdot dt = \phi_{tot} \cdot \frac{\tau \cdot F}{1 + 2 \cdot \tau \cdot F}.$$

The equation that describes the emission anisotropy arising from the cluster is

$$r_{tot} = r_1 \cdot \frac{\phi_j}{\phi_{tot}} + r_{et} \cdot \frac{\phi_k}{\phi_{tot}}$$
$$\quad\quad\quad\quad\quad\quad\quad\quad\quad\quad\quad\quad\quad\quad (9)$$
$$\Rightarrow r_{tot} = r_1 \cdot \left(\frac{1 + \tau \cdot F}{1 + 2 \cdot \tau \cdot F}\right) + r_{et} \cdot \left(\frac{\tau \cdot F}{1 + 2 \cdot \tau \cdot F}\right).$$

Here $r_{tot}$ is the anisotropy from the cluster, and $r_1$ is the anisotropy from the initially excited molecule, (molecule).

$r_{et}$ is the emission anisotropy from the molecule (molecule $k$) in the cluster that is directly excited by electronic energy transfer. Substitution for Förster's transfer rate (Eq. 6), using $R = R_{jk}$, yields

$$r_{tot} = r_1 \frac{1 + (R_o/R)^6}{1 + 2 \cdot (R_o/R)^6} + r_{et} \cdot \frac{(R_o R)^6}{1 + 2 \cdot (R_o R)^6}. \quad (10)$$

For $(R_o/R)^6 \ll 1$, fluorescence emission arises primarily from the initially excited molecule (molecule $j$), and the total anisotropy approaches that of an isolated molecule ($r = r_1$). For the case of $(R_o/R)^6 \gg 1$, both the initially excited molecule and the second molecule in the cluster radiate with equal efficiency, and the total emission anisotropy represents equal contributions from both molecules.

## N ≥3 clusters

For clusters containing three or more interacting molecules, generalization of Eq. 5 to an $N$ molecule cluster yields (see Craver and Knox, 1971)

$$\frac{d\rho_j(t)}{dt} = -\frac{\rho_j(t)}{\tau} - \sum_{k \neq j}^{N} F_{jk} \cdot \rho_j(t) + \sum_{m \neq j}^{N} F_{mj} \cdot \rho_m(t). \quad (11)$$

Here, the first term on the right side describes the excitation decay in the absence of energy transfer. The second term is a sum over all rates of energy transfer from molecule $k$ to all other molecules in the cluster. The final term is a sum of all rates of energy transfer back to molecule $k$. For $N$ interacting molecules, there are $N$ coupled linear differential equations describing the motion and decay of excitation within the system.

Knox developed an elegant matrix approach for calculating the individual quantum yield of a molecule in a cluster directly from the rate equations describing the cluster (Knox, 1968a; Craver and Knox, 1971). We present it here briefly. A $N \times N$ matrix, $\check{G}_{jk}$ is defined where the $jk$th element is given by

$$G_{jk} \equiv -F_{kj} \cdot (1 - \delta_{jk}) + \left(\frac{1}{\tau} + \sum_{m \neq j}^{N} F_{jm}\right) \cdot \delta_{jk}, \quad (12)$$

where $\delta_{jk}$ is the Kronecker delta function. Equation 11 now takes this form:

$$\frac{d\rho_j(t)}{dt} = -\sum_{k=1}^{N} G_{jk} \cdot \rho_k(t). \quad (13)$$

Equation 13 can be solved for $\rho_k(t)$ as the inverse of the matrix $\check{G}_{jk}$, yielding Equation 14:

$$\rho_k(t) = -\sum_{m=1}^{N} (G^{-1})_{km} \cdot \frac{d\rho_k(t)}{dt}. \quad (14)$$

To calculate the individual quantum yield within a cluster of

$N$ molecules, we proceed as before (Eq. 8) by integrating $\rho_k(t)$ from zero to infinity and dividing by $\tau_o$. By letting the temporal boundary conditions be represented as $\Delta\rho_m = \rho_m(\infty) - \rho_m(0)$, the expression for the quantum yield achieves its final general form,

$$\phi_r = \frac{1}{\tau_o} \cdot \int_0^\infty \rho_r(t) \cdot dt = -\frac{1}{\tau_o} \cdot \sum_{m=1}^{N} (G^{-1})_{rm} \cdot \int_0^\infty \frac{d\rho_m(t)}{dt} \cdot dt$$

$$= -\frac{1}{\tau_o} \cdot \sum_{m=1}^{N} (G^{-1})_{rm} \cdot (\rho_m(\infty) - \rho_m(0)) \quad (15)$$

$$\Rightarrow \phi_r = -\frac{1}{\tau_o} \cdot \sum_{m=1}^{N} (G^{-1})_{rm} \cdot \Delta\rho_m$$

$$\Delta\rho_m = \rho_m(\infty) - \rho_m(0).$$

If we set $\Delta\rho_m = -1$ for the initially excited molecule ($m = 1$), and $\Delta\rho_m = 0$ for all other molecules in the cluster ($m \neq 1$), it is now straightforward to calculate the individual quantum yield for all the molecules in the cluster. The individual quantum yield for the initially excited molecule in a general cluster of $N$ molecules is

$$\phi_1 = \frac{(G^{-1})_{11}}{\tau_o}. \quad (16)$$

Recalling that $\phi_{tot} = \tau/\tau_o$, and provided we can replace each individual transfer emission anisotropy ($r_{et}(n)$) with an average value $\langle r_{et} \rangle$, the equation for the emission anisotropy reduces to

$$r_{tot} = r_1 \cdot \frac{\phi_1}{\phi_{tot}} + \sum_{n \neq 1}^{N} r_{et}(n) \cdot \frac{\phi_n}{\phi_{tot}}$$

$$\Rightarrow r_{tot} = r_1 \cdot \frac{\phi_1}{\phi_{tot}} + r_{et} \cdot \left(1 - \frac{\phi_1}{\phi_{tot}}\right) \quad (17)$$

$$r_{tot} = r_1 \cdot \frac{(G^{-1})_{11}}{\tau} + r_{et} \cdot \left(1 - \frac{(G^{-1})_{11}}{\tau}\right).$$

The $\check{G}_{jk}$ matrix and its inverse $(\check{G}^{-1})_{jk}$ for a cluster of two molecules is presented in the Appendix. In addition, we also present there the matrix for a general cluster of $N$ molecules, under conditions where all $N$ molecules in the cluster interact equally ($F_{jk} = F_{jm}$; $F_{jk} = F_{kj}$, for all $j$, $k$, and $m$). The analysis for this problem is analogous to the two-molecule solution, given that $F_{1N} = (N - 1)F$ and $F_{N1} = F$ (Craver and Knox, 1971). Using the $(\check{G}^{-1})_{11}$ values from the two-molecule matrix and the general $N$ molecule matrix, and substituting each into Eq. 16, we obtain the following expressions for the emission anisotropy arising from a cluster of two and a cluster of $N$ molecules:

$$r_2 = r_1 \cdot \frac{(1 + F \cdot \tau)}{(1 + 2 \cdot F \cdot \tau)} + r_{et} \cdot \frac{(F \cdot \tau)}{(1 + 2 \cdot F \cdot \tau)}$$

$$r_N = r_1 \cdot \frac{(1 + F \cdot \tau)}{(1 + N \cdot F \cdot \tau)} + r_{et} \cdot \frac{(N - 1) \cdot (F \cdot \tau)}{(1 + N \cdot F \cdot \tau)}. \quad (18)$$

Note that this solution is identical to the previous one obtained for a cluster of two (Eq. 9).

Fig. 3 shows the emission anisotropy for clusters numbering between one and four (generated for $r_N$; Eq. 18), as a function of mutual separation distance. The data were calculated by assuming that the emission anisotropy for the initially excited molecule $(r_1)$ is equal to the limiting anisotropy of fluorescein labeled melittin (F-melittin) (0.350; see Materials and Methods), and that the average emission anisotropy following homotransfer $(r_{et})$ is equal to zero. We find that the anisotropy remains constant at large separation distances and descends to a lower plateau at mutual separation distances below 0.8 $R_o$. The curves show that emission anisotropy measurements could theoretically be used to distinguish between clusters of different sizes, especially between a cluster of one and two, but including higher order clusters of up to four.

The advantage of using the matrix approach is that it allows us to calculate the emission anisotropy from clusters of various sizes when the molecules in the cluster do not interact equally. For example, we have analyzed the effect of having a two-molecule cluster with two molecules positioned close to one another, and a third molecule positioned farther away (see Fig. 4). When the relative distance among all three molecules falls below approximately $0.8R_o$, the resultant emission anisotropy becomes less sensitive to unequal interactions and assumes a value characteristic for a cluster of three. Apparently, at these close distances there are enough interactions among all three molecules to distribute the excitation energy effectively. Ultimately, each molecule will receive an equal share of the excitation energy. Thus, when interacting molecules are positioned such

that their mutual separation distances fall below $0.8R_o$, the observed emission anisotropy becomes less sensitive to how near each molecule is to one another, and more dependant upon the number of interacting molecules within the cluster.

## Energy transfer with rotational fluorescence depolarization

Although the average lifetime of the cluster does not change with energy transfer, the individual lifetime components may vary. A decrease in the individual component lifetime could effectively increase the total resultant anisotropy from the cluster. To evaluate each lifetime component we substitute for $\rho_j(t)$ (Eq. 14):

$$\tau_j = \frac{\displaystyle\int_0^\infty t \cdot \rho_j(t) \cdot dt}{\displaystyle\int_0^\infty \rho_j(t) \cdot dt} = \frac{-\displaystyle\sum_{m=1}^N (G^{-1})_{jm} \cdot \int_0^\infty t \cdot \frac{d\rho_m(t)}{dt} \cdot dt}{-\displaystyle\sum_{m=1}^N (G^{-1})_{jm} \cdot \int_0^\infty \frac{d\rho_m(t)}{dt} \cdot dt}$$

$$(19)$$

$$= \frac{-\displaystyle\sum_{m=1}^N (G^{-1})_{jm} \cdot \int_0^\infty t \cdot \frac{d\rho_m(t)}{dt} \cdot dt}{-\displaystyle\sum_{m=1}^N (G^{-1})_{jm} \cdot \Delta\rho_m}.$$

The last integral may be integrated by parts. Provided that $\rho_m(t)$ approaches zero sufficiently fast as $t$ approaches
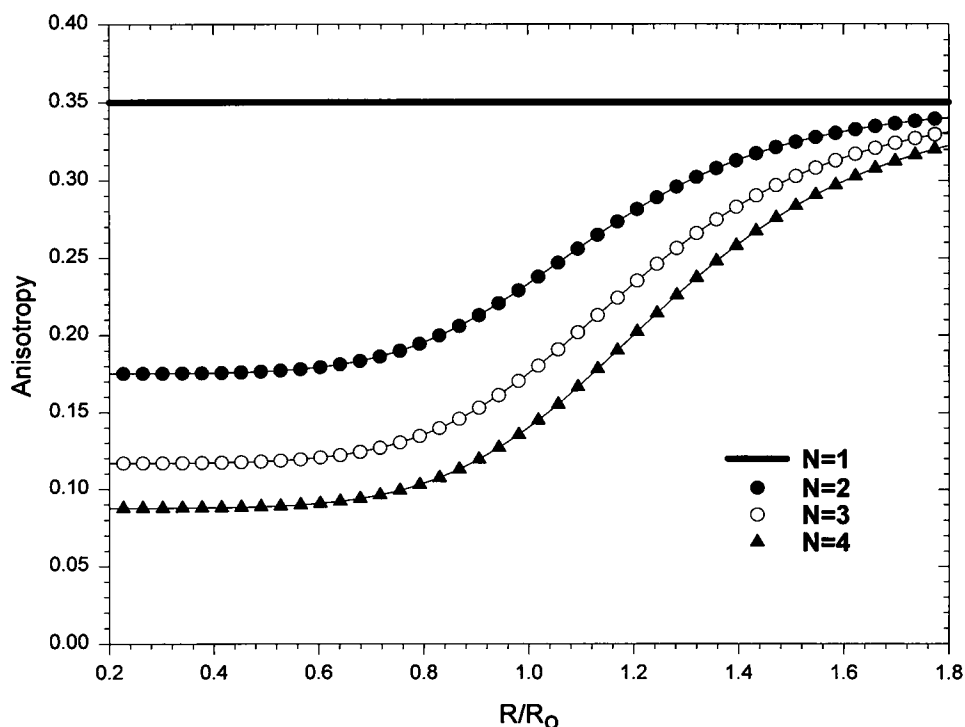


FIGURE 3  Theoretical curves (using Eq. 18 with $r_1 = 0.350$ and $r_{et} = 0$) for the anisotropy emitted from clusters ranging in size from one to four as a function of mutual separation distance. Here the anisotropy of different sized clusters is shown to be clearly distinguishable below $0.8R_o$. In addition, emission anisotropy values remain steady below $0.8R_o$.
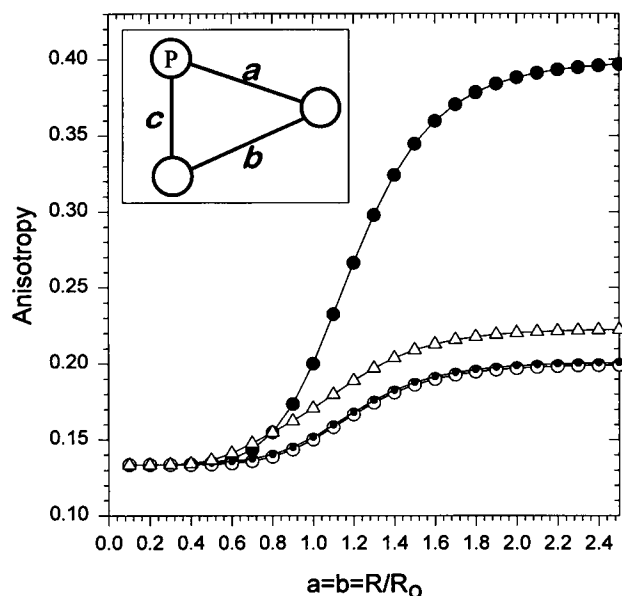
FIGURE 4 These curves show the expected anisotropy from a cluster of two molecules in which a third molecule is added to the cluster at increasingly smaller separation distances to the other two. For these calculations (using Eq. 28; Appendix; with $r_1 = 0.400$ and $r_{et} = 0$) we treated the separation distance between the two molecules in the cluster as constant ($c$), and allowed the distances ($a$ and $b$) to the third molecule from the cluster to vary in length. Here, ⊕ represents the initially photoexcited molecule. (●, : $a = b = c$); (○, $a = b$; $c = 0.1R_o$); (●, $a = b$; $c = 0.5R_o$); (△, : $a = b$, $c = 0.8R_o$). The figure illustrates that these three molecules can interact unequally below mutual separation distances below $0.8R_o$ with the resulting emission anisotropy being the same as if they did interact equally.

infinity, the result is

$$\tau_j = \frac{\sum\limits_{m=1}^{N} (G^{-1})_{jm} \cdot \left( \sum\limits_{n=1}^{N} (G^{-1})_{mn} \cdot \Delta\rho_n \right)}{\sum\limits_{k=1}^{N} (G^{-1})_{jk} \cdot \Delta\rho_k}. \quad (20)$$

The solution to Eq. 20 for a general cluster of $N$ molecules, where all $N$ molecules in the cluster interact equally, is again obtained by assuming that the problem is analogous to the $N = 2$ solution, with $F_{1N} = (N - 1)F$ and $F_{N1} = F$:

$$\tau_1 = \frac{(G^{-1})_{11} \cdot (G^{-1})_{11} + (G^{-1})_{12} \cdot (G^{-1})_{21}}{(G^{-1})_{11}}$$

$$= \tau \cdot \frac{(1 + 2 \cdot \tau \cdot F + N \cdot \tau^2 \cdot F^2)}{((1 + \tau \cdot F) \cdot (1 + N \cdot \tau \cdot F))}. \quad (21)$$

Here $\tau$ is the average lifetime of the cluster, and $\tau_1$ is the individual lifetime of the initially excited molecule (molecule 1).

The emission anisotropy ($r$) of spherical molecule experiencing rotational fluorescence depolarization is given by

the Perrin equation:

$$\frac{1}{r} = \frac{1}{r_o} \cdot \left(1 + \frac{\tau}{\tau_c}\right), \qquad \tau_c = \frac{V \cdot \eta}{k \cdot T} \quad (22)$$

where $\tau_c$ is the rotational correlation time, $V$ is the rotational volume assuming a sphere, $\eta$ is the local viscosity of the solution, $k$ is Boltzmann's constant, $T$ is the temperature, and $r_o$ is the limiting anisotropy (i.e., in the absence of rotational motion). The expression for the anisotropy of the initially excited molecule undergoing both rotational fluorescence depolarization and energy transfer ($r_{1-ET}$) may be written in terms of the anisotropy of the same molecule in the absence of energy transfer ($r_1$). This is accomplished by applying the Perrin equation (Eq. 22) to the change in the lifetime of the initially excited molecule in the presence of energy transfer ($\tau_1$):

$$r_{1-ET} = \frac{r_o}{\left(1 + \frac{\tau_1}{\tau} \cdot \left(\frac{r_o}{r_1} - 1\right)\right)}. \quad (23)$$

If we assume that the initially excited molecule carries the weight of the emission anisotropy (i.e., $r_{et} = 0$) and substitute $r_{1-ET}$ for $r_1$ in Eq. 17, then recalling the general expression for $\tau_1$ (Eq. 20) yields the general equation for the emission anisotropy from a cluster of $N$ molecules corrected for the effect that energy transfer has on the lifetime of the initially excited molecule:

$$r = \frac{r_{1-ET}}{\tau} \cdot (G^{-1})_{11} = \frac{r_o \cdot (G^{-1})_{11}}{\tau \cdot \left(1 + \frac{\tau_1}{\tau} \cdot \left(\frac{r_o}{r_1} - 1\right)\right)},$$

$$\tau_1 = \frac{\sum\limits_{m=1}^{N} (G^{-1})_{1m} \cdot \left( \sum\limits_{n=1}^{N} (G^{-1})_{mn} \cdot \Delta\rho_n \right)}{\sum\limits_{k=1}^{N} (G^{-1})_{1k} \cdot \Delta\rho_k}. \quad (24)$$

When all $N$ molecules interact equally, the above equation reduces to the following simpler form:

$$r = \frac{r_o \cdot \left(\frac{1 + \tau \cdot F}{1 + N \cdot \tau \cdot F}\right)}{\left(1 + \frac{\tau_1}{\tau} \cdot \left(\frac{r_o}{r_1} - 1\right)\right)},$$

$$\frac{\tau_1}{\tau} = \frac{(1 + 2 \cdot \tau \cdot F + N \cdot \tau^2 \cdot F^2)}{((1 + \tau \cdot F) \cdot (1 + N \cdot \tau \cdot F))}. \quad (25)$$

Fig. 5 shows theoretical curves for the emission anisotropy from a cluster of $N$ molecules that interact equally, undergoing energy transfer and rotational motion with and without the lifetime correction term (generated from Eqs. 18 and 25, respectively). The expected values for the emission anisotropy with energy transfer in the absence of the lifetime correction term are shown with dashed lines and small

FIGURE 5 Theoretical curves using $r_1 = 0.200$ and $r_{et} = 0$ for the anisotropy emitted from clusters ranging in size from one to four as a function of mutual separation distance, calculated with (Eq. 25) and without (Eq. 18), a correction for the effect of homotransfer on the individual lifetime of the initially excited molecule undergoing rotational motion. The effects of the perturbed lifetime are not noticeable below $0.8R_o$ but are clearly observable in the transition region $(0.8R_o < R < R_o)$. Dashed curves with large symbols represent theoretical data with the lifetime correction term.
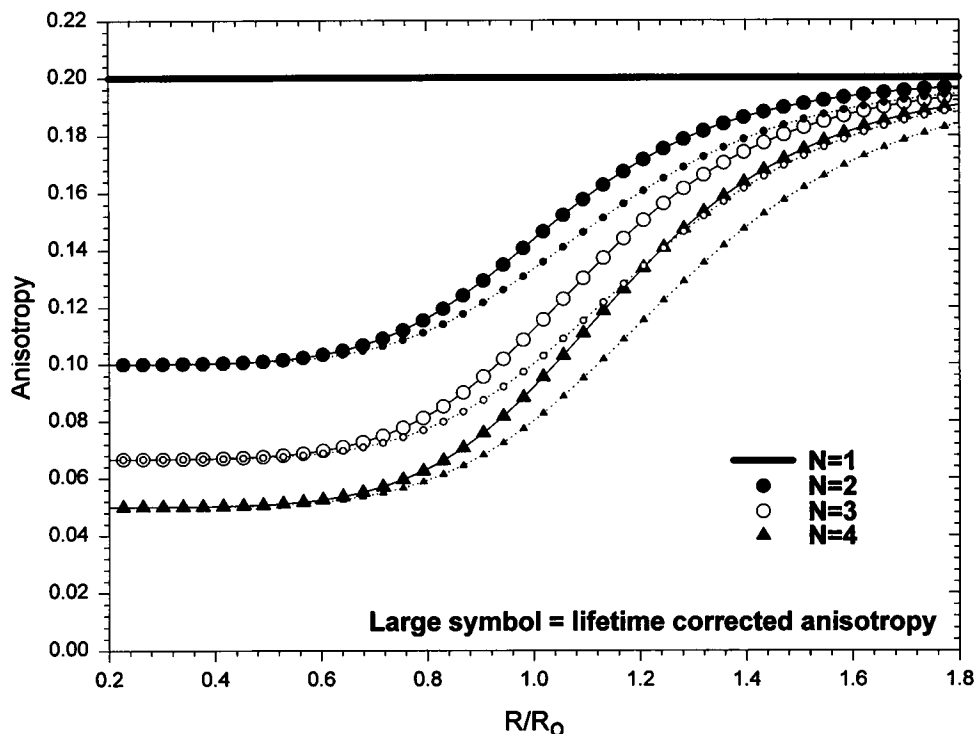


symbols. The larger symbols with solid lines represent the same case with the lifetime correction. Fig. 5 illustrates how the correction term slightly delays the onset of homotransfer fluorescence depolarization, while enhancing the transition to the lower plateau. It is instructive to note that the additional term does not appear to significantly affect emission anisotropy values at mutual separation distances below $0.8R_o$.

## Scope of theory

An exact treatment of homotransfer in macromolecular complexes would require a full vectorial theory, in which individual components of the fluorophore transition moments would be considered. Here we have introduced an approximate scaler formulation that is a physical and generalizable method for constructing working models of mutually interacting fluorophores on proteins or between protein subunits. In addition, we have introduced formulas for analyzing the number of molecules (N) in an arbitrary cluster by measuring three experimental observables ($r_1$, $r_{el}$, and $r_{tot}$; Eq. 18).

As with traditional energy transfer (heterotransfer), the dependence of the transfer rate $(F_{jk})$ on the angular factor $\kappa^2$ is problematic, because the energy transfer efficiency can be extremely sensitive to changes in $\kappa^2$. However, this problem appears to be less significant in homotransfer emission anisotropy measurements when mutual separation distances among the molecules fall below $0.8R_o$ (lower plateaus in Figs. 3 and 5). Within this region the resultant emission anisotropy becomes less sensitive to changes in energy

transfer efficiency, and more dependent upon the number of molecules in the cluster.

## RESULTS AND DISCUSSION

### Effect of methanol on melittin aggregation

In an initial study, we began with melittin tetramers and used methanol to induce dissociation. The rationale behind using methanol is that it preserves the helical structure of the monomers (Lakowicz et al., 1990; Bazzo et al., 1988), and so the addition of methanol will allow us to view the dissociation of $\alpha$-helical tetramers to $\alpha$-helical monomers, without the complication of large changes in secondary structure.

To examine the change in fluorescence anisotropy upon melittin association in the absence of homotransfer, we mixed fluoresceinylated melittin (F-melittin) with native melittin at a 1:24 molar ratio so that each tetramer would have essentially only one labeled species. We began under conditions in which melittin should be tetrameric: 4.63 $\mu$M melittin in 12 mM (2-(N-cyclohexylamino)-ethanesulfonic acid, pH 10.0, and 1.5 M NaCl (Wilcox and Eisenberg, 1992). Methanol was then titrated into solution to induce dissociation. Fig. 6 A (open circles) shows that the anisotropy starts at a high value, undergoes a slight increase, and then quickly falls into a gradually descending slope. Although the underlying reason for the initial increase is unclear and may reflect a small conformational rearrangement of the fluorescein in the melittin tetramer, the decrease
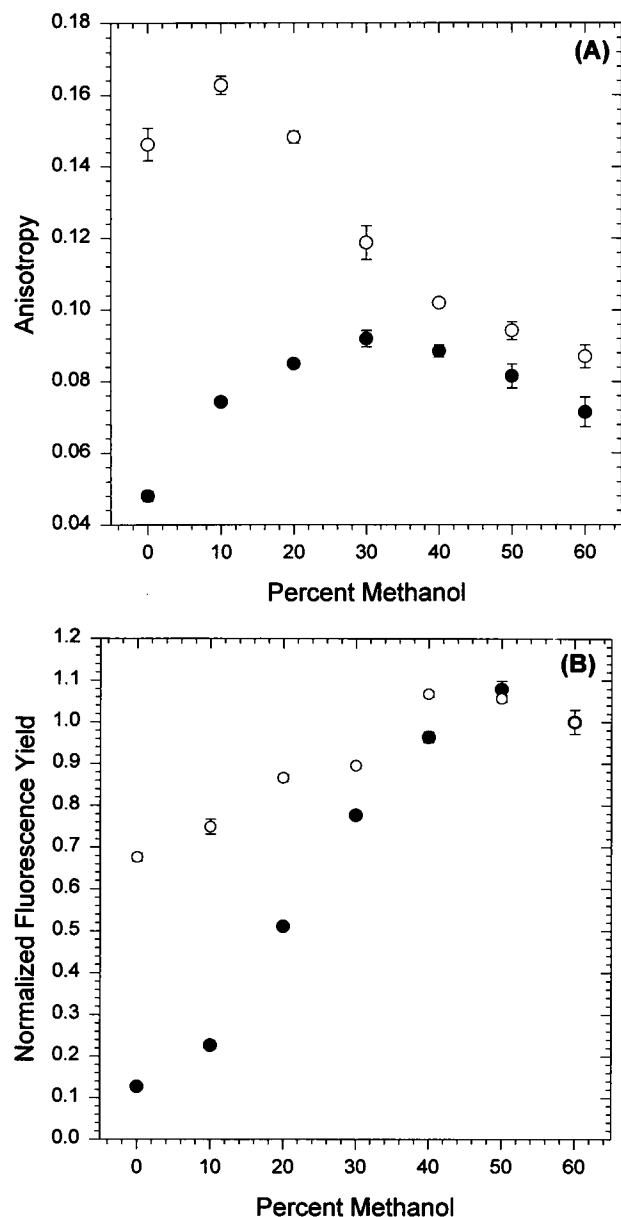
FIGURE 6 (A) Comparison of the anisotropy of 1:24 melittin mixture (O) ([F-melittin] = 185 nM and [native melittin] = 4.44 μM, initially), and 100% F-melittin (●) (4.63 μM, initially) in various percentage methanol (v/v) mixtures, at 1.5 M NaCl, 12 mM CHES, pH 10.0, initially. (B) Comparison of the normalized intensity of 1:24 melittin mixture (O) and 100% F-melittin (●) in various percentage methanol mixtures (v/v), at 1.5 M NaCl, 12 mM CHES, pH 10.0, initially. We normalized the two curves to a value of 1 at 60% methanol.

in anisotropy reflects an average loss in rotational volume as F-melittin:melittin tetramers dissociate to monomers.

An identical study was conducted under conditions in which homotransfer should occur (i.e., 100% F-melittin, initially at 4.63 μM); the results are shown in Fig. 6 A (filled circles). At low methanol concentrations the anisotropy values are far smaller than those seen with 1:24 melittin mixture, indicating the presence of homotransfer within the

F-melittin tetramers. Thus, the excitation energy from the initially excited molecule is communally shared between its neighbors in the cluster, and the resulting emission anisotropy reflects the fraction of the initially excited molecules whose excitation energy has been distributed to its neighbors. As more methanol is added and the tetramers dissociate, homotransfer decreases, and the anisotropy of the 100% F-melittin appears to approach asymptotically the anisotropy of the 1:24 melittin mixture.

The total fluorescence intensity at 520 nm was measured as a function of methanol for both the 1:24 melittin mixture (open circles) and the 100% F-melittin sample (filled circles) (see Fig. 6 B). (The total fluorescence intensity at 520 nm was calculated using $I_{tot} = I_\parallel + 2 \cdot I_\perp$, where $I_\parallel$ and $I_\perp$ are the intensities of vertically and horizontally polarized light.) The intensity of the 1:24 melittin mixture increases with increasing methanol, presumably because of a loss in static quenching from melittin's charged residues as the tetramer dissociates, and because of an increase in quantum yield with increasing methanol. Similarly, the 100% F-melittin intensity also rises with increasing methanol, but to a larger extent than does 1:24 melittin mixture. This shows that self-quenching of the fluorescein residues occurs within the 100% F-melittin tetramers.

## Effect of sodium chloride on melittin aggregation

To verify the sensitivity of fluorescein homotransfer to changes in melittin tetramer-monomer equilibrium, we conducted complementary studies using ionic strength to induce melittin aggregation. Many reports have appeared describing melittin aggregation with increasing ionic strength and at pH values where its amide groups are protonated (Talbot et al., 1979; Brown et al., 1980; Bello et al., 1982; Quay and Condie, 1983; Wilcox and Eisenberg, 1992; Teng and Scarlata, 1993). Fig. 7 A (open circles) shows the aggregation of a 1:24 F-melittin:native melittin mixture (6.93 μM total peptide concentration) in solutions of increasing ionic strength in the absence of homotransfer. When the NaCl concentration is raised from 0.0 to 1.5 M, the anisotropy of the 1:24 melittin mixture drops slightly at 0.25 M NaCl, and then rapidly increases to the higher values that characterize melittin's tetrameric state. (Increasing the molarity of NaCl from 0.0 to 1.5 M increases the bulk viscosity by roughly 15% (Wolf et al., 1980), which accounts for the slight increase in anisotropy at high salt concentrations.) We conducted an analogous experiment under conditions where homotransfer is expected to occur using 100% F-melittin (Fig. 7 A, filled circles). The anisotropy of 100% F-melittin starts at approximately the same value as the 1:24 melittin solution, drops at 0.25 M NaCl, and then remains constant from 0.25 to 1.5 M NaCl. The small difference between the anisotropy values of the two samples at 0 M NaCl reflects the increased tendency of the modified N-terminus melittin to self-associate (see below).

Fig. 7 B shows the total fluorescence intensity at 520 nm for 1:24 mixed melittin (open circles) and 100% F-melittin
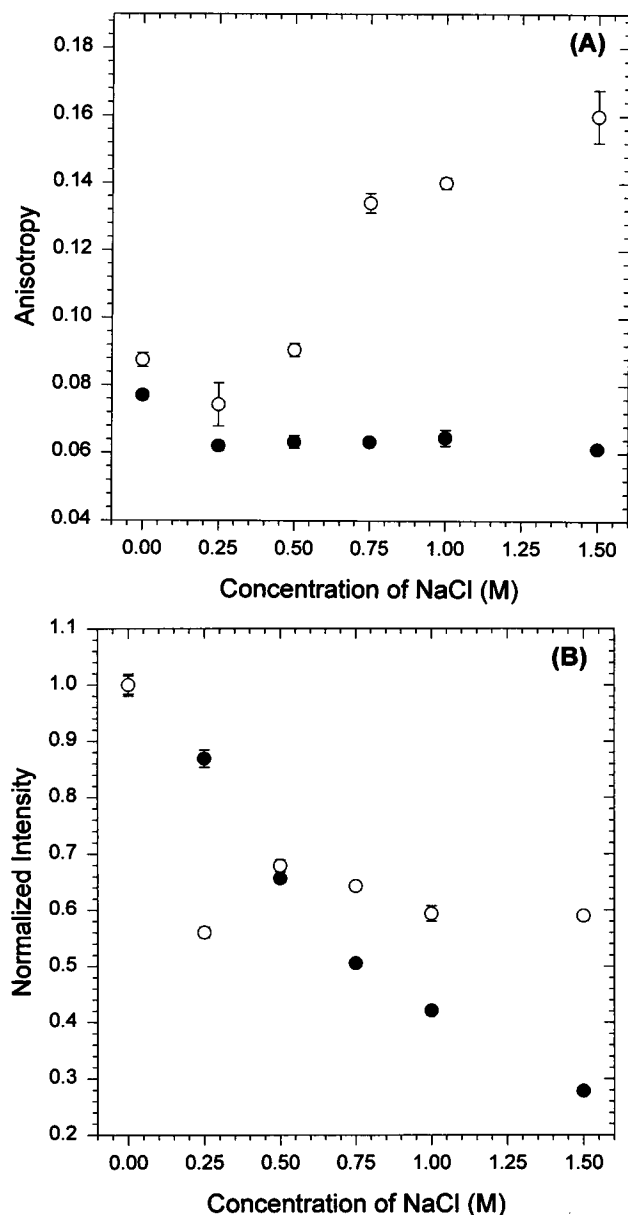
show that self-quenching of the fluorescein moieties is occurring in the F-melittin homotetramers.

With the exception of the anomalous point of the 1:24 mixed melittin at 0.25 M NaCl (Fig. 7 A, open circles), the anisotropy dependence on a monomer to tetramer association with ionic strength is comparable to that observed using methanol. We interpret this anomaly as being due to the preferential self-association of F-melittin at this ionic strength. This interpretation is supported by far-UV circular dichroism studies (Hagihara et al., 1992) and NMR studies (Brown et al., 1980), which have shown that N-terminal derivatized melittin self-associates at a much lower ionic strength than native melittin. In addition, this observation has been substantiated by previous fluorescence studies (Teng and Scarlata, 1993). Because labeling melittin with fluorescein removes a positive charge from the peptide, it is reasonable to expect that the F-melittin species should aggregate at a lower ionic strength.

## Effect of sodium chloride on melittin aggregation in glycerol

To determine the effect of rotational motion on the homotransfer studies, we repeated the sodium chloride experiments in a more viscous solution that will damp rotational motion to some extent. Fig. 8 shows a comparison of the ionic strength dependence of the anisotropy of the 1:24 melittin mixture (open circles) and 100% F-melittin (filled circles) at different ionic strengths in the presence of 50% (v/v) glycerol. Both curves are similar in shape to those
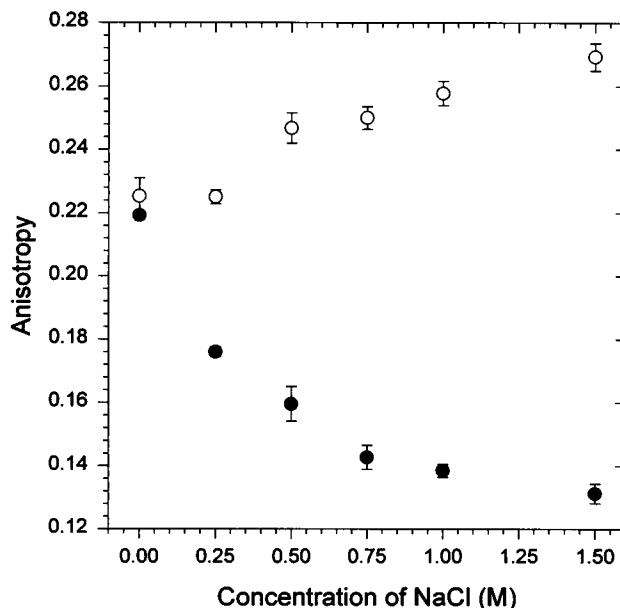
FIGURE 7   (A) Comparison of the anisotropy of 1:24 melittin mixture (○) ([F-melittin] = 277 nM and [native melittin] = 6.65 $\mu$M) and 100% F-melittin (●) (6.93 $\mu$M) with increasing NaCl concentration, 12 mM MOPS, pH 7.2. (B) Comparison of the intensity, normalized at 0 M NaCl, of 1:24 melittin mixture (○) and 100% F-melittin (●) with increasing NaCl concentration, 12 mM MOPS, pH 7.2. Fresh samples were prepared to generate each point.

(filled circles) as a function of increasing ionic strength for NaCl concentrations ranging from 0.0 to 1.5 M. The normalized intensity of the 100% F-melittin samples (filled circles) descends monotonically. In contrast, the intensity of the 1:24 melittin mixture (open circles) drops to a low value at 0.25 M NaCl, increases slightly at 0.50 M NaCl, and then gradually levels. As observed in the methanol studies, the drop in intensity for 100% F-melittin is larger than for the 1:24 melittin mixture upon tetramerization. These data



FIGURE 8   Comparison of the anisotropy of 1:24 melittin mixture (○) ([F-melittin] = 277 nM and [native melittin] = 6.65 $\mu$M) and 100% F-melittin (●) ([F-melittin] 6.93 $\mu$M) with increasing NaCl concentration in 50% (v/v) glycerol, 12 mM MOPS, pH 7.2. Fresh samples were prepared to generate each point.

observed in the absence of glycerol (Fig. 7 A). However, the relative decrease in the emission anisotropy for the 100% F-melittin is not as large. The relative fluorescence yield at 520 nm of both the 100% F-melittin and the 1:24 mixed melittin samples were higher in glycerol, yet the fluorescence intensity of the 100% F-melittin was still lower than with the mixed 1:24 mixed melittin sample. Interpretation of the fluorescence intensity changes is discussed below.

## Effect of membranes on melittin aggregation

The purpose of this series of experiments is to apply homotransfer analysis to the oligomerization of a membrane protein. The binding of melittin to membranes has been extensively studied (Dempsey, 1990). Although the oligomerization of melittin in membranes has been controversial (Dempsey, 1990, and references therein), a recent study that takes into account many experimental complications (John and Jähnig, 1991) showed that in small unilamellar vesicles of dimyristyl phosphatidyl choline, membrane-bound melittin will aggregate above a peptide to lipid mole ratio of 1:200 at 1 M NaCl.

We conducted our studies using large unilamellar vesicles (LUVs) composed of 100% 1-palmitoyl-2-oleoyl-sn-glycero-3-phosphorylcholine (POPC) lipids. Fig. 9 illustrates the results of a series of experiments with POPC LUVs, in which the aggregation state of melittin in membranes was studied as a function of the molar ratio of POPC

lipid to total peptide. All solutions contained 1 M NaCl and 20 mM MOPS, pH 7.2.

We were able to follow melittin's transition from a non-aggregated to aggregated state by examining its ability to form mixed aggregates with fluoresceinylated melittin (F-melittin) at the different lipid:peptide molar ratios (open circles, 1:10 F-melittin:melittin; open squares, 1:15 F-melittin:melittin). Above a lipid:peptide molar ratio of 2000:1, native melittin is unassociated and is unable to form mixed tetramers with F-melittin. In contrast, 100% F-melittin aggregates in POPC membranes at the same lipid:peptide molar ratios (filled circles) apparently remain associated below lipid:peptide molar ratios of approximately 20,000:1 (data not shown). The dip at the end of the 100% F-melittin curve (filled circles) (at low POPC:lipid ratios) is presumably due to homotransfer between the individual F-melittin homoaggregates as mutual separation distances between them approach $R_0$. In addition, our measurements show that changing the F-melittin to native melittin molar ratio to 1:15 (open squares) raises the maximum attainable emission anisotropy. Thus, the 1:10 mixed melittin curve (open circles) of Fig. 9 represents mixed melittin aggregates in which homotransfer is still occurring. Our results show that native melittin begins to aggregate in POPC membranes at lipid:peptide molar ratios below 2000:1. This value is a factor of 10 higher than that obtained by John and Jähnig (1991). Although the reason behind this discrepancy is unclear, we postulate that it is due to a decreased ability of melittin to aggregate on the highly curved surface of small, unilamellar vesicles, as opposed to the flat, uniform surface of large, unilamellar vesicles.

We also conducted potassium iodide (KI) quenching studies with 1:10 mixed melittin to assess the membrane position of the fluorescein label of the melittin aggregate. Under conditions where mixed melittin will aggregate, addition of 1.0 M KI quenches the fluorescence intensity at 520 nm by approximately 78.7 ± 2.5%, whereas KCl decreases the intensity by 26.7 ± 0.7%. Yet in the absence of POPC membranes, 1.0 M KI and 1.0 M KCl treatment of mixed melittin solutions decrease the fluorescence intensity 88.5 ± 1.2% and 6.1 ± 0.8%, respectively. Thus, we estimate that the addition of KI to mixed melittin and POPC lipid solutions, under conditions in which aggregation is expected to occur, quenches the fluorescence intensity at 520 nm by approximately (78.7 − 26.7)/(88.5 − 6.1) × 100, or 63.1%, relative to the solution state tetramer. These data suggest that close to half the fluorescein moieties in the mixed melittin POPC membrane aggregate are on the surface of the membrane's outer leaflet.
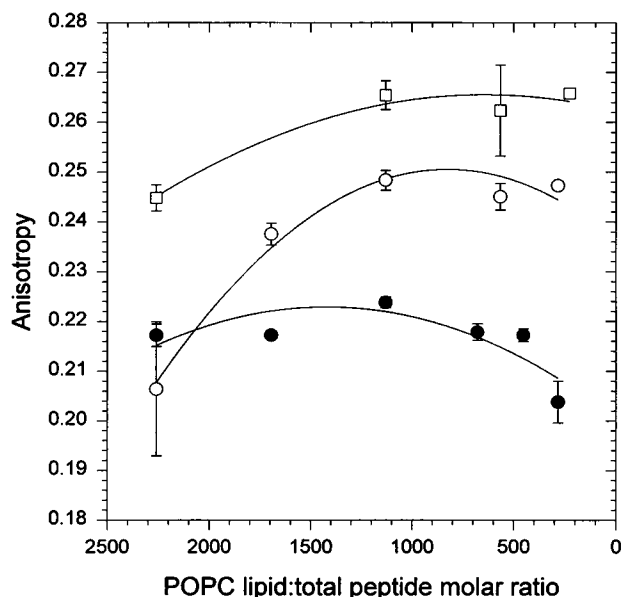


FIGURE 9  Comparison of the anisotropy of 1:10 melittin mixture (○) ([F-melittin] = 250 nM; [melittin] = 2.5 μM), 1:15 melittin mixture (□) ([F-melittin] = 100 nM;[melittin] = 1.5 μM), and 100% F-melittin (●) ([F-melittin] = 2.75 μM) at various POPC lipid to peptide molar ratios. The curves drawn are simply meant to guide the eye and no physical model is implied.

## Fluorescein self-quenching

To further examine the underlying cause of the self-quenching between the fluorescein moieties, we measured the difference in the fluorescence lifetime between the 100% F-melittin tetramers and the 1:24 mixed melittin tetramers.

Preliminary results indicate that the fluorescence lifetime in the 100% F-melittin tetramers is lower than in the 1:24 mixed melittin tetramers for both 1.5 M NaCl, 20 mM MOPS, pH 7.2 (4%), and 1.5 M NaCl, 20 mM MOPS, pH 7.2, in 50% (v/v) glycerol (~13%) aqueous solutions. These small differences in fluorescence lifetime are not nearly large enough to account for the large difference in fluorescence intensity between the F-melittin homotetramers and the 1:24 mixed melittin tetramers. Evidently, static quenching between the fluorescein residues must account for a large portion of the difference. In support of this, we observe that the absorption spectrum of 100% F-melittin is red-shifted with respect to the 1:24 mixed melittin absorption spectrum (data not shown) under conditions in which melittin is expected to be aggregated as tetramers. We interpret this red shift as being due to the absorption by nonfluorescent fluorescein dimers. Chen and Knutson (1988) also observed a red shift in fluorescein absorption, which they attributed to the presence of fluorescein dimers.

Self-quenching of fluorescein has previously been reported and is believed to be a result of two processes: nonfluorescent fluorescein dimer formation and energy transfer from active fluorescein monomers to dark fluorescein dimers (Agranovich and Galanin, 1982, and references therein; Sims and Weidmer, 1984; Chen and Knutson, 1988). Our observation of both dynamic and static quenching in the 100% F-melittin tetramers supports this interpretation. Dark complex formation in the 100% F-melittin tetramers could potentially reduce the number of active neighbors the initially excited molecule has within its cluster (see Fig. 2 c). For a cluster of four in which two of the members have engaged in a dark complex, the anisotropy

would only reflect the excitation energy mixing between the two active fluorophores. This process could possibly account for the decreased quantum yield, the reduced lifetime, and the smaller difference between the anisotropy of 1:24 mixed melittin and the 100% F-melittin tetramer observed with the 50% (v/v) glycerol/sodium chloride experiment.

## Theoretical analysis of homotransfer in F-melittin tetramers

The crystal structure of the melittin tetramer in solution has been solved (Terwilliger and Eisenberg, 1982). Fig. 10 is a cartoon of the melittin tetramer based on its solved crystal structure, with the addition of fluorescein molecules attached to each subunit's Gly-1. Relative separation distances between melittin tetramer's four Gly-1s (A&B&C&D) were calculated and used as an estimate for the relative distances between fluorescein molecules. To compute the inverse $G$ matrix, we first used the estimated separation distances among the fluorescein residues and a $R_o$ value of 53 Å to calculate the theoretical Förster transfer rates (Eq. 6), and then constructed the $G$ matrix elements using Eq. 12 (see Appendix for $G$ matrix and its inverse). Taking the $(G^{-1})_{11}$ element, we calculated the expected emission anisotropy for a F-melittin homotetramer in the above experiments, using Eq. 17 and the approximations $r_{et} = 0.016$, and $r_1 = r_{mixed}$. The value $r_{et} = 0.016$ represents the case for randomly oriented fluorophores (see theory). A summary of the results of these calculations, along with experimental data ($r_{mixed}$ and $r_{100\%}$), are given in Table 1. In addition, we also present the theoretically expected anisot-

FIGURE 10 Sketch of melittin tetramer based on crystal structure (Wilcox and Eisenberg, 1992), with a fluorescein molecule shown attached to each subunit's Gly-1. Relative separation distances between melittin tetramer's four Gly-1s (A&B&C&D) were calculated from the reported crystal structure. These values were used to estimate Förster's bimolecular transfer rate ($F$) between the four fluorescein molecules. The amount of the electronic transfer activity (number of transfers) during an average fluorescence lifetime ($F*\tau$) is illustrated as well.



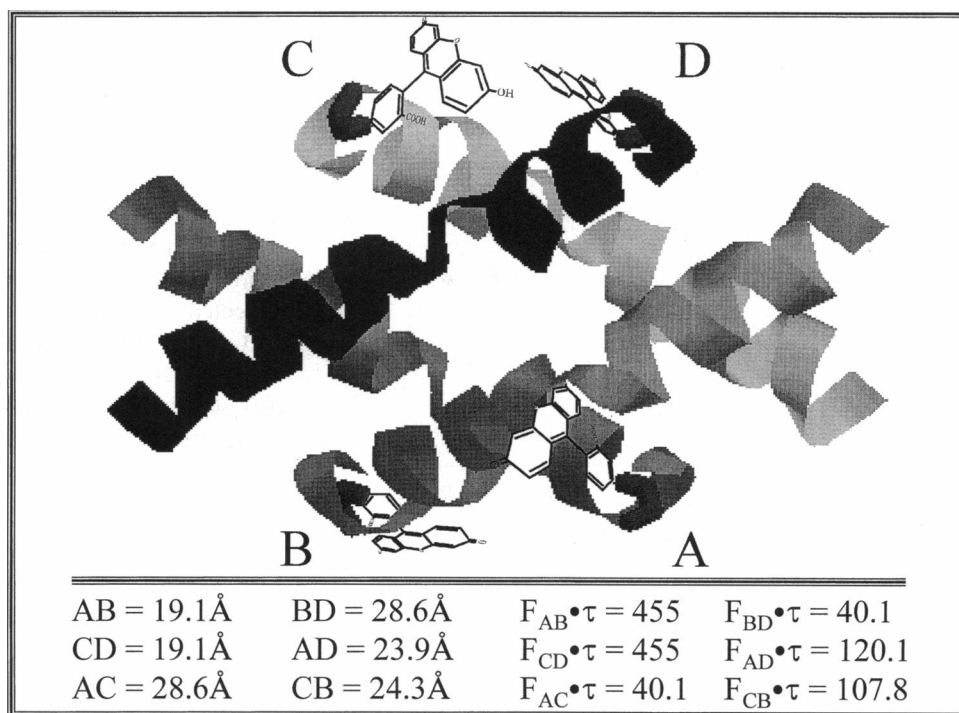| AB = 19.1Å | BD = 28.6Å | $F_{AB} \cdot \tau = 455$ | $F_{BD} \cdot \tau = 40.1$ |
| CD = 19.1Å | AD = 23.9Å | $F_{CD} \cdot \tau = 455$ | $F_{AD} \cdot \tau = 120.1$ |
| AC = 28.6Å | CB = 24.3Å | $F_{AC} \cdot \tau = 40.1$ | $F_{CB} \cdot \tau = 107.8$ |

**TABLE 1   Summary of theoretical analysis for F-melittin studies**

| Sample | $r_{mixed}$ $r_1$ | $r_{100\%}$ $r_{tot}$ | $r_{N=4}$ (Eq. 17) | $r_{N=4}$ (Eq. 18) | $r_{N=2}$ (Eq. 18) |
|---|---|---|---|---|---|
| 0% Methanol | $0.1463 \pm 0.0045$ | $0.0480 \pm 0.0014$ | 0.0487 | 0.0488 | 0.0814 |
| 1.5 M NaCl | $0.1598 \pm 0.0077$ | $0.0613 \pm 0.0005$ | 0.0521 | 0.0522 | 0.0882 |
| 1.5 M NaCl + 50% glycerol | $0.2693 \pm 0.0043$ | $0.1313 \pm 0.0031$ | 0.0796 | 0.0797 | 0.1432 |
| 400:1 POPC:F-mel and 500:1 POPC:mixed mel in 1.0 M NaCl | $0.2623 \pm 0.0091$ | $0.2172 \pm 0.0013$ | 0.0779 | 0.0780 | 0.1397 |

$r_{mixed}$ and $r_{100\%}$ are the experimental anisotropy values for 1:24 F-melittin: native melittin and 100% F-melittin. $r_{N=4}$ (Eq. 17) is the theoretical anisotropy value assuming nonequal interacting species, and $r_{N=4}$ and $r_{N=2}$ (Eq. 18) are the theoretical anisotropy value assuming equal interactions for clusters of 4 and 2, respectively. For these calculations we assigned $r_{mixed}$ to $r_1$ and used a value 0.016 for $r_{et}$. Setting $r_{et}$ equal to 0.016 represents the case in which the fluorophores' dipole moments are randomly distributed with respect to each other (see theory).

ropy using Eq. 18, assuming an average mutual separation distance of 23.94 Å between the fluorophores in the F-melittin homotetramer. Because the mutual separation distances between the fluorescein residues in the F-melittin homotetramer are smaller than $0.8R_o$, the theoretical expected anisotropy calculated assuming nonequal interactions (Eq. 17) is nearly identical to the result calculated assuming equal interactions (Eq. 18). For comparison, we also calculated the expected emission anisotropy from a cluster of two fluorophores, again assuming an average mutual separation distance of 23.94 Å between the two fluorophores.

We find that the theory predicts an anisotropy for $N = 4$ that is close to what is experimentally observed for both the methanol and the nonglycerol/NaCl experiments. However, for the 50% (v/v) glycerol/NaCl case, the experimentally observed anisotropy more closely resembles what would be expected for an $N = 2$ cluster. Interestingly, the agreement between the anisotropy values for the NaCl/glycerol experiment and the theoretical values calculated for an $N = 2$ cluster supports the idea that viscous solvents stabilize the formation of dark fluorescein dimers, which reduces the active number of fluorophores in the F-melittin homotetramers from four to two. However, this view would have to be substantiated by ruling out that a high $r_{et}$ value in glycerol does not account for the apparent discrepancy. To that end, we are currently conducting experiments to test the validity of setting $r_{et} = 0.016$ in the above analysis (see Materials and Methods).

Our analysis of the POPC membrane experiments show that fluorescence depolarization in the F-melittin homoaggregate lies above what we would expect for the anisotropy from a cluster of two or four. (In these calculations we assumed the structure of the F-melittin homoaggregates in membranes is similar to the structure of the melittin tetramer in solution, with two fluorescein moieties on either side of the homoaggregate. This view is supported by the KI quenching study, where half of the fluorescence is quenched by adding quencher to the outside of the membranes.) However, in our theoretical evaluation we assumed that $r_{et} = 0.016$. The fluorescein moieties within the F-melittin homoaggregate in POPC membranes may be rotationally restricted, which could possibly raise the $r_{et}$ value. In addi-

tion, fluorescein dimer formation within the F-melittin homoaggregate may also contribute the high anisotropy values. The key point in this study is that homotransfer is capable of detecting the protein association of the membrane-bound peptide. However, it is unclear whether our data reflect a monomer to dimer equilibrium or monomer to higher order oligomer equilibrium. Studies are under way to address this point.

## CONCLUSIONS

In this study we have described a general theory of fluorescence depolarization in clusters of randomly orientated fluorophores. We have explicitly shown that the extent of fluorescence depolarization is proportional to the number of fluorophores within the cluster. A formalism was also described to correct for the effect of energy transfer on the individual lifetime of the initially excited molecule.

Below the critical mutual separation distance $(R_o)$, changes in the number of molecules within a cluster are resolvable. It is possible, as we have shown for melittin, to use homotransfer analysis to monitor changes in oligomerization states greater than a monomer to dimer, or to observe protein-protein associations where more than two proteins are involved, in solution and in membranes.

Below approximately $0.8R_o$, homotransfer analysis has the potential to be used as an analytical tool to determine the number of subunits in an oligomer. We have shown that at these close distances there is sufficient transfer activity within the cluster to distribute the excitation energy among the members of the cluster evenly, including cases in which the fluorophores do not interact equally. Thus, when mutual separation distances fall below $0.8R_o$, the anisotropy from non-uniform fluorophore distributions is nearly equal to the anisotropy for an idealized isometric distribution.

Our initial results support the use of homotransfer analysis to monitor changes in subunit oligomerization, and as a qualitative measure of the number of subunits in a cluster. However, our results also show that more detailed work is needed to make this method quantitative. These studies are currently under way.

## APPENDIX

The $G$ matrix and its inverse for the $N = 2$ cluster, and for a general cluster of $N$ with $F_{12} = (N - 1)F$ and $F_{21} = F$, are

$$\check{G}_{kn}(N = 2) = \begin{bmatrix} 1/\tau + F_{12} & -F_{21} \\ -F_{12} & 1/\tau + F_{21} \end{bmatrix}, \qquad \check{G}_{kn}(N) = \begin{bmatrix} 1/\tau + (N - 1) \cdot F & -F \\ -(N - 1) \cdot F & 1/\tau + F \end{bmatrix} \qquad (26)$$

$$(\check{G}^{-1}(N = 2))_{mn} = \begin{bmatrix} \dfrac{(1 + F \cdot \tau) \cdot \tau}{(1 + 2 \cdot F \cdot \tau)} & \dfrac{F \cdot \tau^2}{(1 + 2 \cdot F \cdot \tau)} \\ \dfrac{F \cdot \tau^2}{(1 + 2 \cdot F \cdot \tau)} & \dfrac{(1 + F \cdot \tau) \cdot \tau}{(1 + 2 \cdot F \cdot \tau)} \end{bmatrix}, \qquad (\check{G}^{-1}(N))_{mn} = \begin{bmatrix} \dfrac{(1 + F \cdot \tau) \cdot \tau}{(1 + N \cdot F \cdot \tau)} & \dfrac{F \cdot \tau^2}{(1 + N \cdot F \cdot \tau)} \\ \dfrac{(N - 1) \cdot F \cdot \tau^2}{(1 + N \cdot F \cdot \tau)} & \dfrac{(1 + (N - 1) \cdot F \cdot \tau) \cdot \tau}{(1 + N \cdot F \cdot \tau)} \end{bmatrix} \qquad (27)$$

The equation for the emission anisotropy for the $N = 3$ cluster (Eq. 28) was derived by first constructing the $G$ matrix, taking its inverse, and setting $r_{et} = 0$. The solution for the quantum yield from the initially excited molecule in a cluster of three was obtained by Knox (Craver and Knox, 1971):

$$r = r_1 \cdot \frac{1 + \tau \cdot (F_{12} + F_{13} + 2 \cdot F_{23}) + \tau^2 \cdot (F_{12} \cdot F_{13} + F_{12} \cdot F_{23} + F_{13} \cdot F_{23})}{1 + 2 \cdot \tau \cdot (F_{12} + F_{13} + F_{23}) + 3 \cdot \tau^2 \cdot (F_{12} \cdot F_{13} + F_{12} \cdot F_{23} + F_{13} \cdot F_{23})}, \quad F_{ij} = F_{jk}; \quad r_{et} = 0 \qquad (28)$$

The $G$ matrix and its inverse for the F-melittin tetramer were calculated by assuming that the mutual separation distances between N-terminally linked fluorophores are equal to the separation distances between the four Gly-1 residues in the crystal structure of the melittin tetramer, and by using an $R_0$ of 53 Å (Terwilliger and Eisenberg, 1982).

$$\check{G} = \begin{bmatrix} \dfrac{1}{\tau} + \dfrac{(455 + 107.82 + 40.13)}{\tau} & \dfrac{-455.00}{\tau} & \dfrac{-107.82}{\tau} & \dfrac{-40.13}{\tau} \\ \dfrac{-455.00}{\tau} & \dfrac{1}{\tau} + \dfrac{(455 + 40.12 + 120.08)}{\tau} & \dfrac{-40.13}{\tau} & \dfrac{-120.08}{\tau} \\ \dfrac{-107.82}{\tau} & \dfrac{-40.12}{\tau} & \dfrac{1}{\tau} + \dfrac{(107.82 + 40.12 + 454.78)}{\tau} & \dfrac{-454.78}{\tau} \\ \dfrac{-40.13}{\tau} & \dfrac{-120.08}{\tau} & \dfrac{-454.78}{\tau} & \dfrac{1}{\tau} + \dfrac{(40.13 + 120.08 + 454.78)}{\tau} \end{bmatrix} \qquad (29)$$

$$\check{G}^{-1} = \tau \cdot \begin{bmatrix} 0.25115 & 0.25019 & 0.24906 & 0.24901 \\ 0.25019 & 0.25111 & 0.24901 & 0.24909 \\ 0.24906 & 0.24901 & 0.25115 & 0.25019 \\ 0.24901 & 0.24909 & 0.25019 & 0.25111 \end{bmatrix} \qquad (30)$$

The formula for the individual component lifetime of the initially excited molecule for a cluster of four was calculated using Eq. 20:

$$\tau_1 = \frac{(G^{-1})_{11} \cdot (G^{-1})_{11} + (G^{-1})_{12} \cdot (G^{-1})_{21} + (G^{-1})_{13} \cdot (G^{-1})_{31} + (G^{-1})_{14} \cdot (G^{-1})_{41}}{(G^{-1})_{11}} \qquad (31)$$

## REFERENCES

Agranovich, V. M., and M. D. Galanin. 1982. *Electronic Excitation Energy Transfer in Condensed Matter.* North-Holland Publishing, New York.

Bazzo, R., M. J. Tappin, A. Pastore, T. S. Harvey, J. A. Carver, and I. D. Campbell. 1988. The Structure of melittin. A $^1$H-NMR study in methanol. *Eur. J. Biochem.* 173:139–146.

Bello, J., H. R. Bello, and E. Granados. 1982. Conformation and aggregation of melittin: dependence on pH and concentration. *Biochemistry.* 21:461–465.

Brown, L. R., J. Lauterwein, and K. Wüthrich. 1980. High resolution $^1$H-NMR studies of self-aggregation of melittin in aqueous solution. *Biochim. Biophys. Acta.* 622:231–244.

Cantor, C. R., and P. R. Schimmel. 1980. *Biophysical Chemistry II: Techniques for the Study of Biological Structure and Function.* W. H. Freedom and Co., San Francisco.

Casey, J. R., and R. A. F. Reithmeier. 1991. Analysis of the oligomeric state of band 3, the anion transport protein of the human erythrocyte membrane, by size exclusion high performance liquid chromatography.

Oligomeric stability and origin of heterogeneity. *J. Biol. Chem.* 266: 15726–15737.

Chen, R. F., and J. R. Knutson. 1988. Mechanism of fluorescence concentration quenching of carboxyfluorescein in liposomes: energy transfer to nonfluorescent dimers. *Anal. Biochem.* 172:61–77.

Craver, F. W., and R. S. Knox. 1971. Theory of polarization quenching by excitation transfer II. Anisotropy and second-neighbour considerations. *Mol. Phys.* 22:385–402.

Dempsey, C. E. 1990. The actions of melittin on membranes. *Biochim. Biophys. Acta.* 1031:143–161.

Erijman, L., and G. Weber. 1991. Oligomeric protein associations: transition from stochastic to deterministic equilibrium. *Biochemistry.* 30: 1595–1599.

Faucon, J. F., J. Dufourcq, and C. Lussan. 1979. The self-association of melittin and its binding to lipids: an intrinsic fluorescence polarization study. *FEBS Lett.* 102:187–190.

Förster, T. 1993. Intermolecular energy migration and fluorescence. *In* Biological Physics. E. V. Mielczarek, E. Greenbaum, R. S. Knox, editors. American Institute of Physics, New York.

Goto, Y., and Y. Hagihara. 1992. Mechanism of the conformational transition of melittin. *Biochemistry.* 31:732–738.

Hagihara, Y., M. Kataoka, S. Aimoto, and Y. Goto. 1992. Charge repulsion in the conformational stability of melittin. *Biochemistry.* 31: 11908–11913.

Haugland, R. P. 1992. *Handbook of Fluorescent Probes and Research Chemicals*. K. D. Larison, editor. Molecular Probes, Inc., Eugene, OR.

Herbert, D. N., and A. Carruthers. 1991. Cholate-solubilized erythrocyte glucose transporters exists as a mixture of homodimers and homotetramers. *Biochemistry*. 30:4654–4658.

Herbert, D. N., and A. Carruthers. 1992. Glucose Transporter oligomeric structure determines transporter function. Reversible redox-dependent interconversion of tetrameric and dimeric GLUT1. *J. Biol. Chem.* 267: 23829–23838.

John, E., and F. Jähnig. 1991. Aggregation state of melittin in lipid vesicle membranes. *Biophys. J.* 60:319–328.

Knox, R. S. 1968a. On the theory of trapping of excitation in the photosynthetic unit. *J. Theor. Biol.* 21:244–259.

Knox, R. S. 1968b. Theory of polarization quenching by excitation transfer. *Physica*. 39:361–386.

Lakowicz, J. R., I. Gryczynski, W. Wiczk, G. Laczko, F. C. Prendergast, and M. L. Johnson. 1990. Conformational distributions of melittin in water/methanol mixtures from frequency-domain measurements of nonradiative energy transfer. *Biophys. Chem.* 35:99–115.

Lauterwein, J., L. R. Brown, and K. Wüthrich 1980. High resolution ¹H-NMR studies of monomeric melittin in aqueous solution. *Biochim. Biophys. Acta*. 622:219–230.

Quay, S. C., and C. C. Condie. 1983. Conformational studies of aqueous melittin: thermodynamic parameters of the monomer-tetramer self-association reaction. *Biochemistry*. 22:695–700.

Sims, P. J., and T. Wiedmer. 1984. Kinetics of polymerization of a fluoresceinated derivative of complement protein C9 by the membrane-bound complex of complement proteins C5b-8. *Biochemistry*. 23: 3260–3267.

Steinberg, I. Z. 1971. Long-range nonradiative transfer of electronic excitation energy in proteins and polypeptides. *Annu. Rev. Biochem.* 40: 83–114.

Talbot, J. C., J. Dufourcq, J. de Bony, J. F. Faucon, and C. Lussan. 1979. Conformational change and self association of monomeric melittin. *FEBS Lett.* 102:191–193.

Teng, Q., and S. Scarlata. 1993. Effect of high pressure on the association of melittin to membranes. *J. Biol. Chem.* 268:12434–12442.

Terwilliger, T. C., and D. Eisenberg. 1982. The structure of melittin. I. Structure determination and partical refinement. *J. Biol. Chem.* 257: 6010–6015.

Timmins, P. A., and G. Zaccai. 1988. Low resolution structures of biological complexes studied by neutron scatter. *Eur. Biophys. J.* 15:257–268.

Voss, J., L. R. Jones, and D. D. Thomas. 1994. The physical mechanism of calcium pump regulation in the heart. *Biophys. J.* 76:190–196.

Weber, G., and E. Daniels. 1966. Cooperative effects in binding by bovine serum albumin. II. The binding of 1-anilino-8-napthalenesulfonate. Polarization of the ligand fluorescence and quenching of the protein fluorescence. *Biochemistry*. 5:1900–1907.

Weber, G., and F. W. J. Teale. 1957. Determination of the absolute quantum yield of fluorescent solutions. *Faraday Soc. Trans.* 53: 646–655.

Wilcox, W., and D. Eisenberg. 1992. Thermodynamics of melittin tetramerization determined by circular dichroism and implications for protein folding. *Protein Sci.* 1:641–653.

Wolf, A. V., M. G. Brown, and P. G. Prentiss. 1980. Concentrative properties of aqueous solutions: conversion tables. *In* Handbook of Chemistry and Physics. R. C. Weast, editor. CRC Press, Boca Raton, FL.